JOC The Journal of Organic Chemistry

pubs.acs.org/joc Article

Immobilization of Trifluoromethyl-Substituted Pyridine-Oxazoline Ligand and Its Application in Asymmetric Continuous Flow Synthesis of Benzosultams

Martin Kocúrik, Jan Bartáček,* Pavel Drabina, Jiří Váňa, Jan Svoboda, Lenka Husáková, Vladimír Finger, Michaela Hympánová, and Miloš Sedlák

Cite This: J. Org. Chem. 2023, 88, 15189−15197 Read Online

ACCESS | Metrics & More | Article Recommendations | Supporting Information

ABSTRACT: This study presents an improved synthetic route to ligand (*S*)-4-(*tert*-butyl)-2-(5-(trifluoromethyl)pyridin-2-yl)-4,5-dihydrooxazole and its application as a highly active and enantioselective catalyst in the addition of arylboronic acids to cyclic *N*-sulfonylketimines. Immobilization of such a ligand was achieved using a commercially available starting material and a PS−PEG TentaGel S NH_2 support, resulting in a stable heterogeneous catalyst. Although the anchored catalyst exhibited a slight reduction in enantioselectivity and a 4-fold decrease in reaction rate, it displayed remarkable stability, enabling 10 consecutive reaction cycles. Furthermore, the successful transition to a continuous flow system demonstrated even higher turnover numbers compared to batch arrangements. These findings provide valuable insights into the development of efficient flow reactors for continuous synthesis of benzosultams, further advancing the field of asymmetric catalysis.

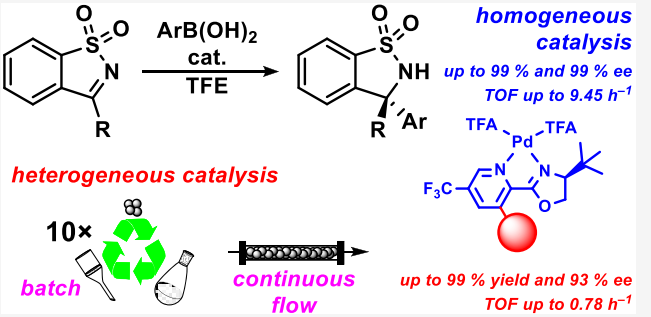

INTRODUCTION

Pyridine-oxazoline (PyOx) type ligands are widely recognized for their privileged role in asymmetric catalysis by transition metal complexes. Their extensive applicability has been extensively reviewed.[1,2] Electronic properties play a crucial role in their effectiveness, and among the electron-poor ligands, those featuring trifluoromethyl (**L1**) or methoxycarbonyl (**L2**) groups at the 5-position of the pyridine ring are frequently employed (Figure 1). The first advantage of **L1** over **L2** lies in its convenient synthesis from readily available precursors, making it attractive for large-scale syntheses. Pd complexes of **L1** have demonstrated utility in various reactions including conjugated addition of boronic acids to enones,[3] redox-relay Heck reactions,[4−9] Heck−Matsuda arylation,[10,11] arylboration,[12] and several Heck-related cascade reactions.[13,14] Additionally, the Cu(I) complex of **L1** has been employed as a catalytic system for conjugate addition to isocyanoalkenes,[15] Ni(I) complex for hydroalkynylation,[16] and Ni(0) complex for asymmetric reductive coupling.[17] In addition, analogous ligands featuring different substitutions at the oxazoline moiety and maintaining the trifluoromethyl group at the 5-position of the pyridine ring have been employed in various catalytic transformations.[18−27]

On the other hand, the synthesis of ligand **L2** is more laborious and provides lower yields.[28] Nevertheless, it has been found to be a valuable ligand in the preparation of optically enriched cyclic sulfonamides containing a bis-benzylic

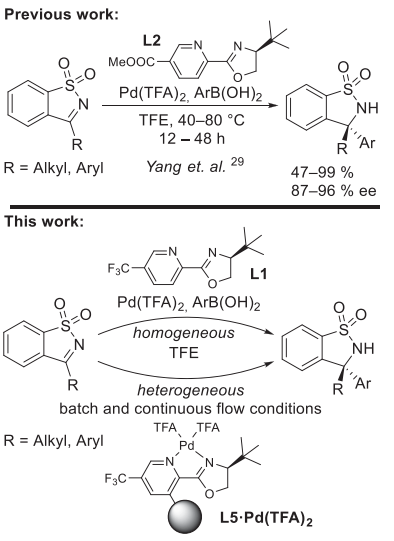

Figure 1. Aim of the work and previous work.

Received: July 26, 2023
Published: October 12, 2023

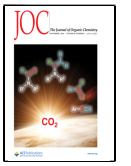

https://doi.org/10.1021/acs.joc.3c01671
J. Org. Chem. 2023, 88, 15189−15197

Scheme 1. Optimized Synthesis of L1

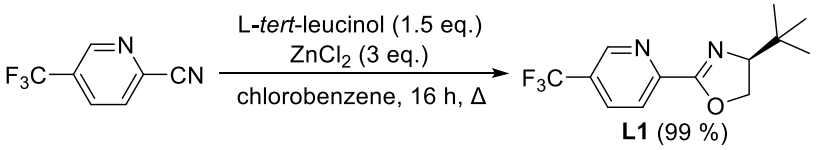

quaternary stereogenic center through the addition of arylboronic acids to saccharin-derived cyclic ketimines[29] (Scheme 1). The addition of boronic acids to cyclic *N*-sulfonylketimines has been extensively studied under Pd catalytic conditions,[29−36] as well as with other transition metals such as Rh, Ni, or Co.[37] The resulting products, sulfonamides bearing a quaternary stereogenic center, have been utilized for the synthesis of biologically active tertiary amines,[38,39] sulfinyl hydroxylamines,[40] or subjected to further transformations such as heterocyclic ring expansion.[41] Moreover, these compounds, known as benzosultams, exhibit interesting biological properties[42] and can serve as valuable chiral auxiliaries in organic synthesis.[43] Hence, this work aims to investigate the possibility of using the more readily accessible ligand **L1** for the synthesis of this intriguing class of compounds.

Considering the potential of benzosultams as pharmaceutically relevant compounds and their possible synthesis on a large scale, it is worth exploring their synthesis using continuous flow reactors. Flow reactors necessitate catalyst immobilization and the development of synthetic protocols under heterogeneous conditions.

Previous studies have successfully reported immobilization strategies for various pyridine-oxazoline type ligands[44−48] (Figure 2). However, most investigations have primarily focused on immobilizing the unsubstituted pyridine-oxazoline skeleton. The 6-position on the pyridine ring has been employed as an anchoring site for reactions that require a bulky PyOx ligand, such as allylic substitution[44] and cyclopropanation.[45] Alternatively, the 4-position has been utilized for the conjugated addition of arylboronic acids to cyclic enones.[46] Another approach involves anchoring via the 5-position of the oxazoline ring through an ester bond, enabling the preparation of micellar nanoreactors for the conjugated addition of arylboronic acids to chromones.[47,48]

Based on the findings of these prior works, we have designed an immobilization strategy for the available **L1** ligand and aim to test it under heterogeneous batch and continuous flow conditions, which constitutes the second objective of this study.

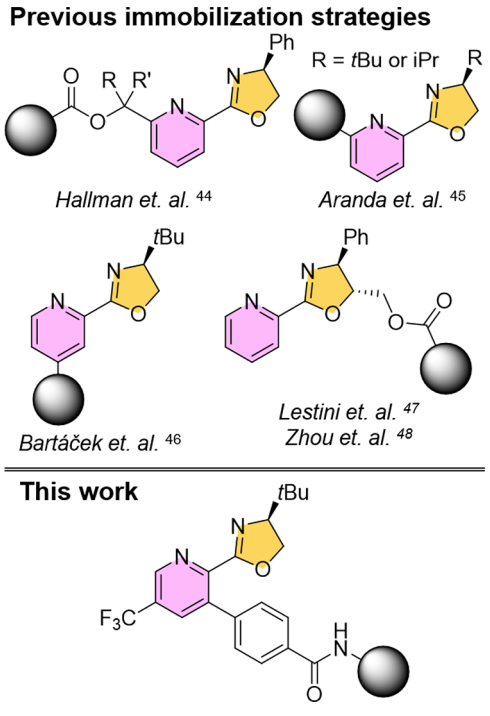

Figure 2. Immobilization strategies for PyOx-type ligands.[44−48]

RESULTS AND DISCUSSION

Homogeneous Catalysis. Initially, we focused on optimizing the synthesis of ligand **L1**. Previous literature[49] reported a 71% yield for the condensation reaction of 5-(trifluoromethyl)picolinonitrile with L-*tert*-Leucinol using 20 mol % $Zn(OTf)_2$ catalyst. However, when this condensation was performed under 300 mol % of $ZnCl_2$ catalysis, ligand **L1** was obtained in nearly quantitative yield (Scheme 1).

To assess the effectiveness of ligand **L1** in comparison to the previously published **L2**, we conducted reactions using various arylboronic acids with 3-butylbenzo[*d*]isothiazole 1,1-dioxide (**S1**) under conditions similar to the original protocol,[29] with a reaction time of 12 h. If complete conversion was not achieved within 12 h, we extended the reaction time to 24 h. For reactions that achieved complete conversion within 12 h, we monitored the reaction at shorter intervals to determine the exact time required for complete conversion.

The results (Figure 3) indicated that the presence of electron-donating groups on arylboronic acids in the meta- and para-positions accelerated the reaction. The highest turnover frequency (TOF) was observed when 4-hydroxyphenylboronic acid was used (Figure 3; **P1l**). However, when we further increased the electron-donating character using 4-(dimethylamino)phenylboronic acid, we observed only minimal conversion (<14%) and the major product was the protodeboronation product *N*,*N*-dimethylaniline within the temperature range of 5−40 °C (Figure 4; **P1r**). The reactivity was significantly reduced for boronic acids with electron-withdrawing substituents such as 3-methoxyphenylboronic acid (Figure 3; **P 1d**) and 4-fluorophenylboronic acid (Figure 3; **P1e**), and the reaction with 3,5-dimethoxyphenylboronic acid was even more sluggish (Figure 4; **P1q**). *Ortho*-substituted boronic acids presented the greatest challenge as the reactivity was fundamentally limited by *ortho* substitution with a methyl or methoxy group, and this limitation could not be compensated even with an electron-donor at position 4- (Figure 4; **P1n**, **P1o**, **P 1p**).

Interestingly, the product of addition of 2-hydroxyphenylboronic acid was isolated in unexpectedly high yield and enantioselectivity (Figure 3; **P1h**). We assume that this is due to possible hydrogen bond formation, which is not possible in the case of methyl or methoxy substitution. However, DFT

https://doi.org/10.1021/acs.joc.3c01671
J. Org. Chem. 2023, 88, 15189−15197

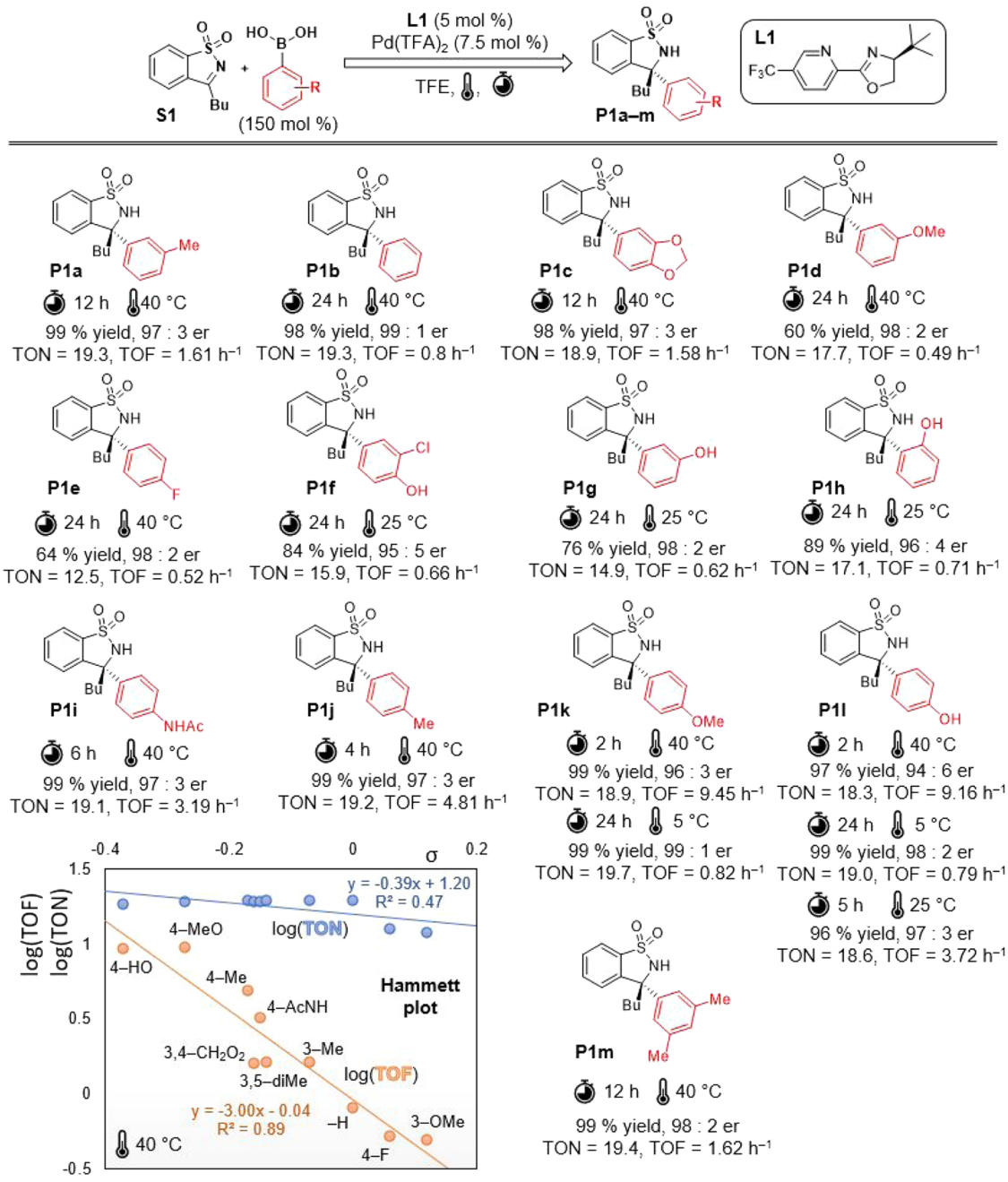

Figure 3. Results of homogeneous catalysis using ligand **L1**.

calculations based on known energy profiles[34] suggest that the transition state of the rate-determining step does not prefer the formation of hydrogen bonds (for more details, see S3).

The negative ρ-value and the overall reactivity trend (Figure 3) suggested that stabilizing the arylpalladium cation with electron donors was advantageous in the rate-limiting step. These findings were consistent with the proposed mechanism, which postulated that migratory insertion is both the rate-determining and enantioselectivity-determining step.[34]

Furthermore, we expanded the substrate scope to include variously substituted ketimines (S2–4) in addition reactions with 4-hydroxyphenylboronic and 4-methoxyphenylboronic acids (Figure 5). High reactivity and enantioselectivity were observed except for the substrate bearing an isopropyl group (S4).

Immobilization Strategy. Immobilization strategy is based on commercially available 3-chloro-5-(trifluoromethyl)-picolinonitrile, which is a precursor for the fungicide fluopicolide.[50] By condensing it with L-*tert*-leucinol, we obtain **L3** bearing a reactive chlorine atom, which was then substituted by a 4-methoxycarbonylphenyl group (**L3a**) through a Suzuki-Miyaura cross-coupling reaction (Scheme 2). Subsequently, **L4a** was hydrolyzed to yield free carboxylic acid (**L4b**). The actual anchoring onto the polymeric carrier was accomplished through amidation between **L4b** and commercially available PS–PEG resin (TentaGel S NH_2), which is generally suitable as a carrier for reactions in a highly polar environment.[51]

From the prepared polymer-supported ligand **L5**, its complex with palladium(II) trifluoroacetate **L5·Pd(TFA)$_2$**

https://doi.org/10.1021/acs.joc.3c01671
J. Org. Chem. 2023, 88, 15189–15197

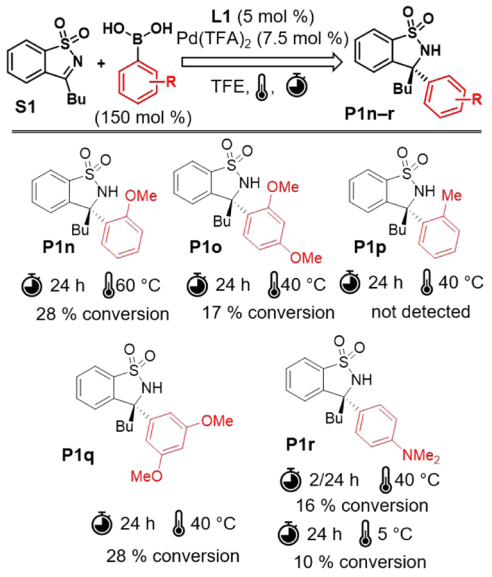

Figure 4. Less successful and unsuccessful results of catalysis using **L1**.

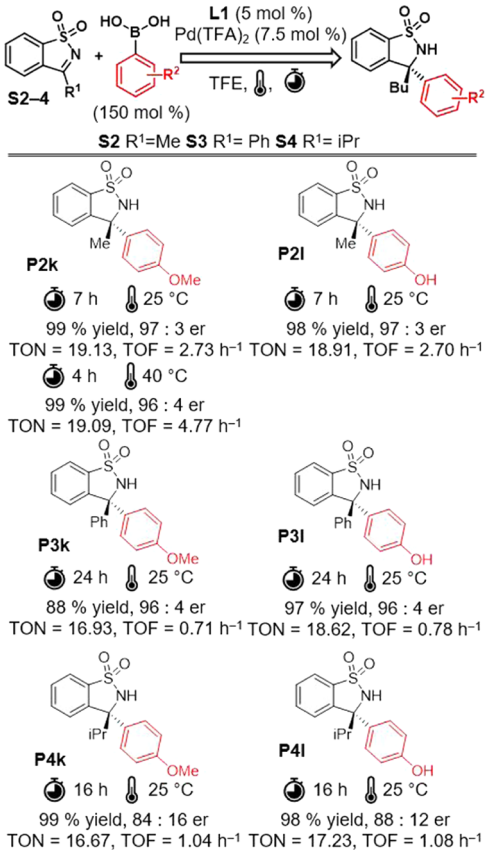

Figure 5. Substrate scope of variously substituted cyclic ketimines.

was prepared (Scheme 2). Ethyl acetate was the solvent of choice due to the limited solubility of $Pd(TFA)_2$ in other organic solvents.

The prepared **L5** was characterized by using FT-IR spectroscopy, microanalysis, and gel-phase ^1H and ^{13}C NMR. The ligand's anchoring is observable in the IR spectra due to the appearance of new amide vibration bands (Figure 6b). The TentaGel resin's swelling properties (Figure 6c) allowed for gel-phase NMR measurements, further supporting the structure of **L5** (Figure 6a). After complexation reaction with $Pd(TFA)_2$, the prepared **L5·Pd(TFA)$_2$** was further characterized using FT-IR spectroscopy (Figure 6b). A change in the infrared spectra is particularly noticeable in the signals corresponding to both the C═O and C−F vibrations (Figure 6b). The exact Pd content was determined through ICP-MS analysis.

Testing the Catalytic Performance of L5·Pd(TFA)$_2$ in Batch Arrangement. After successfully synthesizing the polymer-supported complex **L5·Pd(TFA)$_2$**, its effectiveness for addition reaction of 4-methoxyphenylboronic acid to ketimine **S1** was studied with a focus on its reusability in repeated reaction cycles (Figure 7).

The results revealed that immobilization led to a reduction in the catalytic reaction rate, necessitating a 4-fold increase in reaction time (from 2 to 8 h) and an increase in the loading of the catalyst from 5 to 15 mol % to achieve yields comparable to those obtained with homogeneously catalyzed reactions (Figure 7). At the same time, a slight decrease in the level of observed enantioselectivity was evident. After each reaction cycle, the catalyst was filtered, washed, and used again. It was possible to use the catalyst up to 10 times; however, a slight deactivation of the catalyst was observed with continued recycling cycles. This can be explained by Pd leaching, where the Pd content decreased by 10% during the 10 uses compared with the Pd content of the freshly prepared **L5·Pd(TFA)$_2$** complex.

Thus, the efficiency of the prepared **L5·Pd(TFA)$_2$** on the model reaction can be expressed as TON ∼ 59 and TOF 0.75 h^{-1}, while TON ∼ 19 and TOF = 9.45 h^{-1} were obtained for catalysis in an analogous homogeneous system.

A study of the catalytic properties of **L5·Pd(TFA)$_2$** on a series of substrates was also carried out. While the trend of reactivity was generally the same as in the homogeneous environment, a 4-fold increase in reaction time and 3-fold increase in catalyst loading was required to achieve a conversion comparable to the homogeneous catalysis conditions. The results of Hammett correlation analysis are analogous to a reaction catalyzed in a homogeneous environment (see S4).

Testing the Catalytic Performance of L5·Pd(TFA)$_2$ in Continuous Flow Arrangement. After optimizing the conditions for performing the reaction under batch conditions, we focused on the assessment of the catalytic performance of **L5·Pd(TFA)$_2$** in a continuous flow arrangement. To simulate the continuous flow system, we prepared a reactor column by pressurizing swollen **L5·Pd(TFA)$_2$**. Mechanical pressing using a piston and dosing pump was used to pressurize the column. Prior to use, the column was saturated in solvent to ensure optimum polymer swelling.

Operating at higher pressures compared with the batch experiments was essential in establishing tight contact between the polymer and the reactor tube wall. It prevented the desorption of dissolved oxygen in the reaction mixture, ensuring a consistent catalytic performance. Maintaining a steady pressure in the column was crucial to preventing oxygen desorption and local drying of the polymer, which could hinder catalytic reactions. Thus, saturating the mixture of starting materials with pressure before entering the pump was necessary to facilitate oxygen dissolution and the pump-filling process.

https://doi.org/10.1021/acs.joc.3c01671
J. Org. Chem. 2023, 88, 15189−15197

Scheme 2. Synthetic Pathway to Polymer Supported Pyridine-Oxazoline Ligand L5 and Its Complex L5·Pd(TFA)$_2$

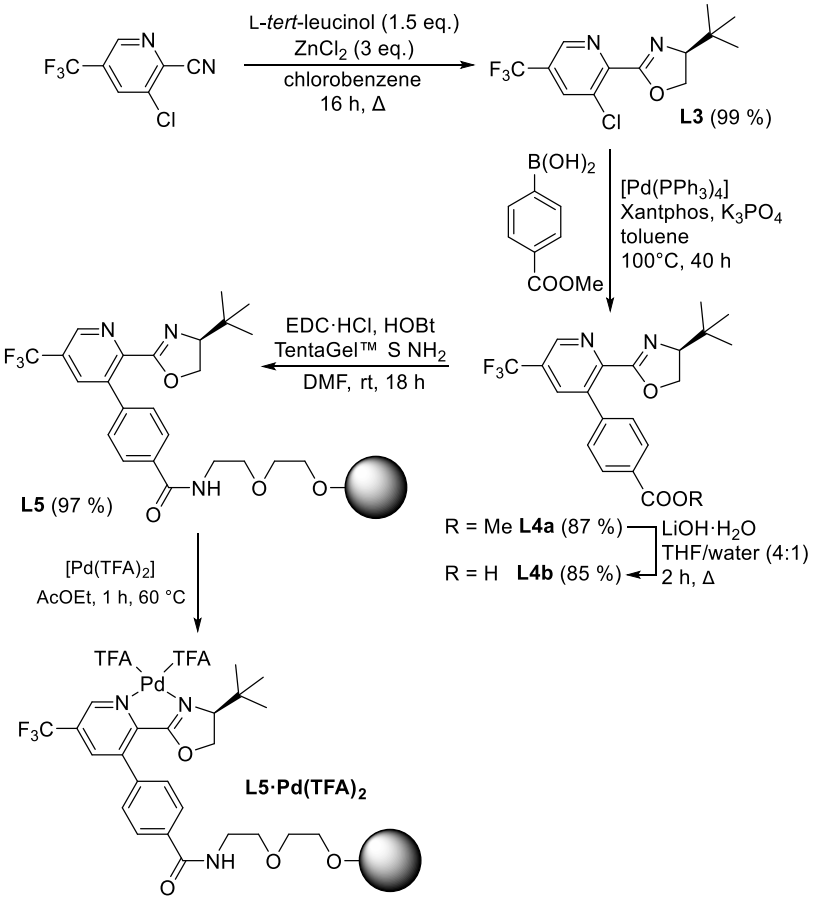

To avoid desorption of oxygen in the pump and subsequent flow stoppage, it was important to ensure the pressure saturation of the mixture in the reservoir. The flow rate of the reaction mixture through the reactor was optimized based on desired conversion and pressure. Increasing the flow rate resulted in higher pressure, facilitating diffusion of reactants into the swelling polymer. This pressure-induced diffusion advantage provided a notable improvement over that of the batch system.

Flow system parameters were optimized to achieve 95+ % conversion of **S1** to **P1j** (see S5 for more details). The optimized conditions obtained were used to conduct the synthesis of **P1j** under continuous flow conditions (Figure 8). During the 143 h experimental period, the prepared **L5·Pd(TFA)$_2$** exhibited an efficiency of TON ∼ 73 and TOF 0.51 h^{-1}. Comparing batch and continuous flow conditions, we observed higher catalyst efficiency under flow conditions (Table 1).

However, there was a slight decrease in the reaction rate (TOF) in the continuous flow system. Notably, the continuous flow setup allowed for a 65% reduction in the usage of TFE.

CONCLUSIONS

In conclusion, this work has presented an improved synthetic route to the ligand (*S*)-4-(*tert*-butyl)-2-(5-(trifluoromethyl)-pyridin-2-yl)-4,5-dihydrooxazole (**L1**) and its successful utilization as a catalyst in the addition of arylboronic acids to cyclic *N*-sulfonylketimines. The ligand **L1**, in the form of a complex with palladium(II) trifluoroacetate, demonstrated high catalytic activity and enantioselectivity, showcasing its potential as a valuable tool in asymmetric synthesis.

Moreover, an immobilization strategy for ligand **L1** was developed using a commercially available starting material and a PS−PEG TentaGel S NH$_2$ type support, leading to the preparation of a heterogeneous catalyst. Although a 4-fold slowing of the reaction rate and a slight reduction in enantioselectivity were observed after anchoring, the immobilized catalyst exhibited remarkable stability, allowing for 10 consecutive reaction cycles. Furthermore, the successful transfer of the reaction to a continuous flow arrangement proved to be highly advantageous, as the immobilized catalyst achieved an even higher turnover number compared with the batch system.

Notably, the flow-through system exhibited an overall longer lifetime of the catalyzing polymer, potentially attributed to its gradual deactivation along the flow direction. In contrast to a batch system where uniform deactivation occurs, the polymer in the flow column experienced greater inactivation at the entrance, while remaining partially active toward the end. Consequently, the turnover frequency (TOF) should be considered as an average value that continuously varies throughout the column.

Overall, this study not only presents a novel synthetic route and an immobilization strategy for ligand **L1** but also demonstrates the efficacy of the catalyst in both batch and continuous flow systems. The findings provide valuable insights into the development of efficient flow reactors for the continuous synthesis of enantioenriched compounds, such

https://doi.org/10.1021/acs.joc.3c01671
J. Org. Chem. 2023, 88, 15189−15197

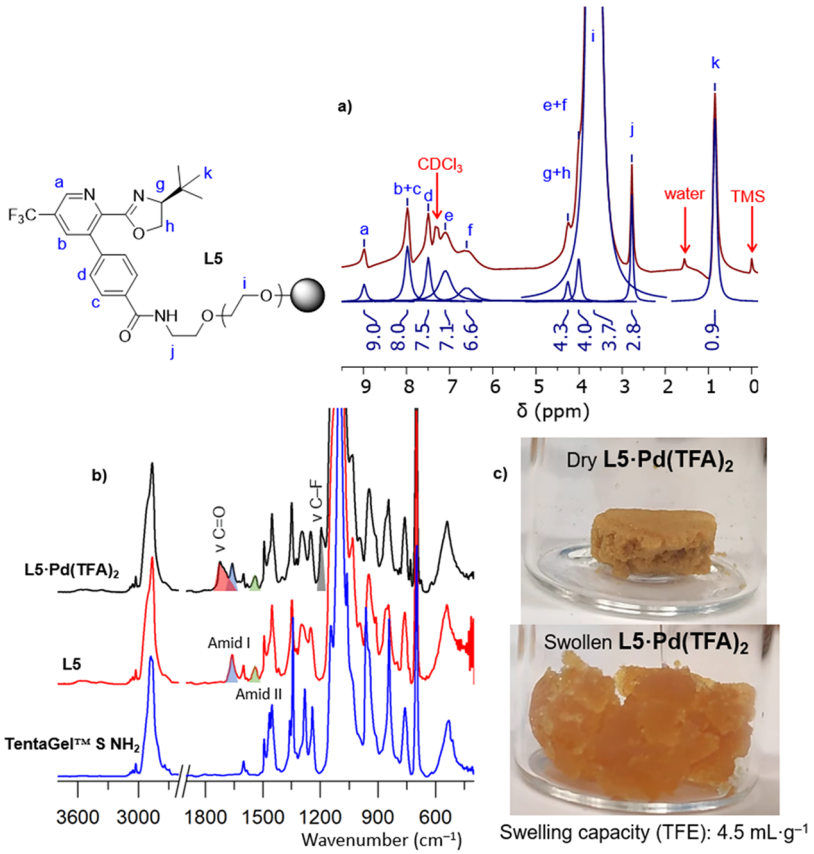

Figure 6. (a) ^{1}H gel-phase NMR of **L5** (b) FT-IR spectra of commercial resin, **L5** and its complex **L5·Pd(TFA)$_2$** (c) photography of dry and swollen **L5·Pd(TFA)$_2$**.

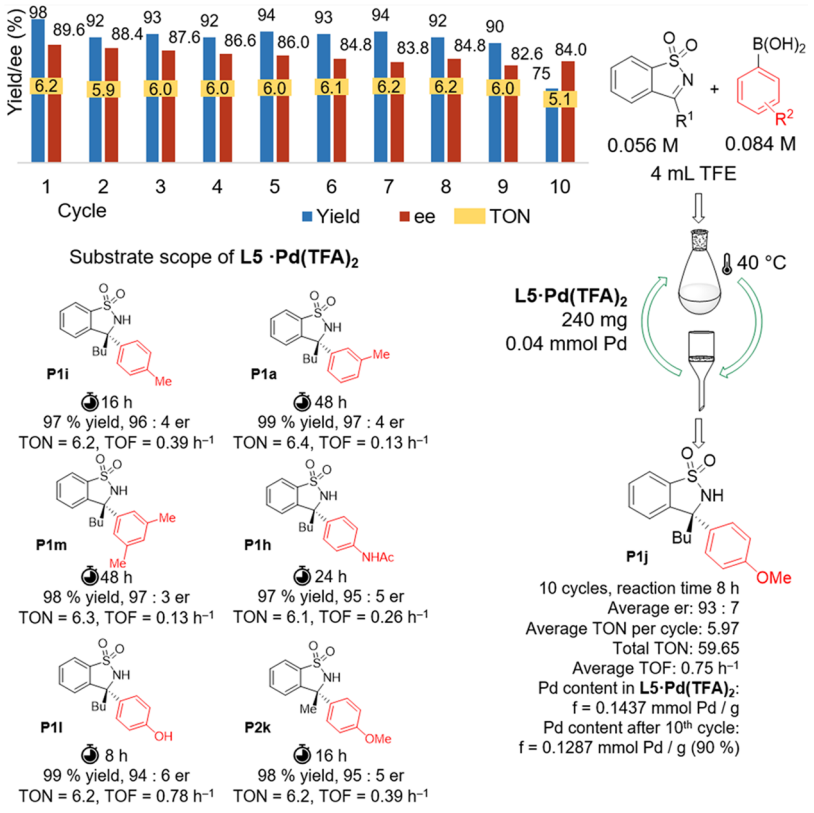

Figure 7. Results of catalytic experiments with **L5·Pd(TFA)$_2$** in batch arrangement.

https://doi.org/10.1021/acs.joc.3c01671
J. Org. Chem. 2023, 88, 15189−15197

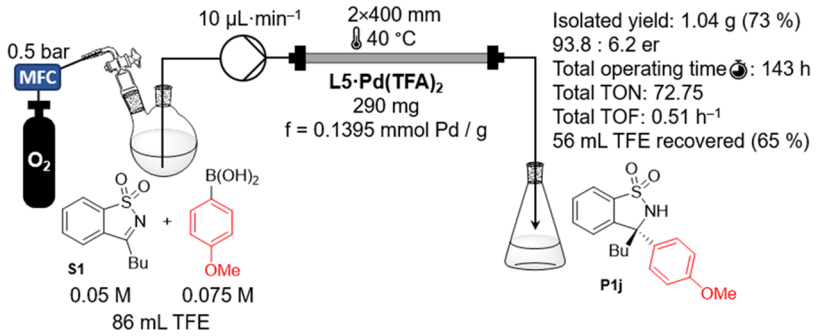

Figure 8. Schematic view and result summarization of continuous flow synthesis of **P1j**.

Table 1. Comparison of Homogeneous and Heterogeneous Catalysis Efficiency

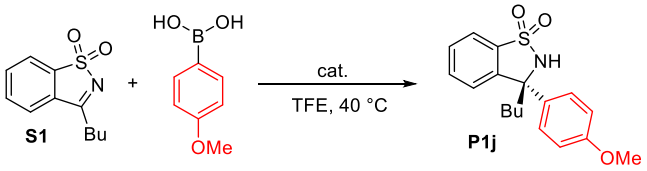

	catalyst		
	L1 + $Pd(TFA)_2$	**L5**·$Pd(TFA)_2$ (batch)	**L5**·$Pd(TFA)_2$ (continuous flow)
e.r.	95.5:4.5	92.9:7.1	93.8:6.2
ee	91	85.8	87.6
TON (−)	18.90	56.56	72.75
TOF (h^{-1})	9.45	0.71	0.51

as benzosultams, and pave the way for further advancements in the field of asymmetric catalysis.

■ ASSOCIATED CONTENT

Data Availability Statement

The data underlying this study are available in the published article and its Supporting Information.

Supporting Information

The Supporting Information is available free of charge at https://pubs.acs.org/doi/10.1021/acs.joc.3c01671.

Experimental details, computational details, HPLC traces, NMR and FT-IR spectra of all the compounds (PDF)

■ AUTHOR INFORMATION

Corresponding Author

Jan Bartáček − *Institute of Organic Chemistry and Technology, Faculty of Chemical Technology, University of Pardubice, Pardubice, CZ 532 10, Czech Republic;* orcid.org/0000-0001-5078-7751; Email: jan.bartacek@upce.cz

Authors

Martin Kocúrik − *Institute of Organic Chemistry and Technology, Faculty of Chemical Technology, University of Pardubice, Pardubice, CZ 532 10, Czech Republic*

Pavel Drabina − *Institute of Organic Chemistry and Technology, Faculty of Chemical Technology, University of Pardubice, Pardubice, CZ 532 10, Czech Republic;* orcid.org/0000-0003-1861-8979

Jiří Váňa − *Institute of Organic Chemistry and Technology, Faculty of Chemical Technology, University of Pardubice, Pardubice, CZ 532 10, Czech Republic*

Jan Svoboda − *Institute of Organic Chemistry and Technology, Faculty of Chemical Technology, University of Pardubice, Pardubice, CZ 532 10, Czech Republic;* orcid.org/0000-0001-7948-4746

Lenka Husáková − *Department of Analytical Chemistry, Faculty of Chemical Technology, University of Pardubice, Pardubice, CZ 532 10, Czech Republic*

Vladimír Finger − *Faculty of Pharmacy in Hradec Králové, Charles University, Hradec Králové, CZ 500 05, Czech Republic; Biomedical Research Center, University Hospital Hradec Králové, Hradec Králové, CZ 500 05, Czech Republic*

Michaela Hympánová − *Biomedical Research Center, University Hospital Hradec Králové, Hradec Králové, CZ 500 05, Czech Republic; Faculty of Military Health Sciences, University of Defence, Hradec Králové, CZ 500 01, Czech Republic*

Miloš Sedlák − *Institute of Organic Chemistry and Technology, Faculty of Chemical Technology, University of Pardubice, Pardubice, CZ 532 10, Czech Republic*

Complete contact information is available at: https://pubs.acs.org/10.1021/acs.joc.3c01671

Author Contributions

The manuscript was written through contributions of all authors. All authors have given approval to the final version of the manuscript.

Notes

The authors declare no competing financial interest.

■ ACKNOWLEDGMENTS

The authors would like to thank the University of Pardubice for their financial support and acknowledge the assistance of ChatGPT for language corrections in the preparation of this manuscript.

■ REFERENCES

(1) Yang, G.; Zhang, W. Renaissance of Pyridine-Oxazolines as Chiral Ligands for Asymmetric Catalysis. *Chem. Soc. Rev.* **2018**, *47* (5), 1783−1810.

(2) Giofrè, S.; Molteni, L.; Beccalli, E. M. Asymmetric Pd(II)-Catalyzed C−O, C−N, C−C Bond Formation Using Alkenes as Substrates: Insight into Recent Enantioselective Developments. *Eur. J. Org. Chem.* **2023**, *26* (2), No. e202200976.

(3) Lamb, C. J. C.; Vilela, F.; Lee, A.-L. Pd(II)-Catalyzed Enantioselective Desymmetrization of Polycyclic Cyclohexenediones: Conjugate Addition versus Oxidative Heck. *Org. Lett.* **2019**, *21* (21), 8689−8694.
(4) Hsu, D.-S.; Wang, M.-Y.; Huang, J.-Y. Asymmetric Total Syntheses of (+)-5-Epi-Schisansphenin B and the Proposed Structure of (+)-15-Hydroxyacora-4(14),8-Diene. *J. Org. Chem.* **2022**, *87* (1), 644−651.
(5) Chen, G.; Cao, J.; Wang, Q.; Zhu, J. Desymmetrization of Prochiral Cyclopentenes Enabled by Enantioselective Palladium-Catalyzed Oxidative Heck Reaction. *Org. Lett.* **2020**, *22* (1), 322−325.
(6) Chen, Z.-M.; Liu, J.; Guo, J.-Y.; Loch, M.; DeLuca, R. J.; Sigman, M. S. Palladium-Catalyzed Enantioselective Alkenylation of Alkenylbenzene Derivatives. *Chem. Sci.* **2019**, *10* (30), 7246−7250.
(7) Yuan, Q.; Sigman, M. S. Palladium-Catalyzed Enantioselective Relay Heck Arylation of Enelactams: Accessing α,β-Unsaturated δ-Lactams. *J. Am. Chem. Soc.* **2018**, *140* (21), 6527−6530.
(8) Jiang, Z.-Z.; Gao, A.; Li, H.; Chen, D.; Ding, C.-H.; Xu, B.; Hou, X.-L. Enantioselective Synthesis of Chromenes via a Palladium-Catalyzed Asymmetric Redox-Relay Heck Reaction. *Chem. − Asian J.* **2017**, *12* (24), 3119−3122.
(9) Zhang, C.; Tutkowski, B.; DeLuca, R. J.; Joyce, L. A.; Wiest, O.; Sigman, M. S. Palladium-Catalyzed Enantioselective Heck Alkenylation of Trisubstituted Allylic Alkenols: A Redox-Relay Strategy to Construct Vicinal Stereocenters. *Chem. Sci.* **2017**, *8* (3), 2277−2282.
(10) Herrera, C. L.; Santiago, J. V.; Pastre, J. C.; Correia, C. R. D. In Tandem Auto-Sustainable Enantioselective Heck-Matsuda Reactions Directly from Anilines. *Adv. Synth. Catal.* **2022**, *364* (11), 1863−1872.
(11) de Oliveira Silva, J.; Angnes, R. A.; Menezes da Silva, V. H.; Servilha, B. M.; Adeel, M.; Braga, A. A. C.; Aponick, A.; Correia, C. R. D. Intermolecular Noncovalent Hydroxy-Directed Enantioselective Heck Desymmetrization of Cyclopentenol: Computationally Driven Synthesis of Highly Functionalized Cis-4-Arylcyclopentenol Scaffolds. *J. Org. Chem.* **2016**, *81* (5), 2010−2018.
(12) Zou, C.; Wu, H.; Ji, Y.; Zhang, P.; Cui, H.; Huang, G.; Zhang, C. Palladium-Catalyzed Intramolecular Dehydrogenative Arylboration of Alkenes. *Chin. J. Chem.* **2022**, *40* (20), 2437−2444.
(13) He, Y.-P.; Cao, J.; Wu, H.; Wang, Q.; Zhu, J. Catalytic Enantioselective Aminopalladation−Heck Cascade. *Angew. Chem., Int. Ed.* **2021**, *60* (13), 7093−7097.
(14) Sun, M.; Wu, H.; Xia, X.; Chen, W.; Wang, Z.; Yang, J. Asymmetric Palladium-Catalyzed C−H Functionalization Cascade for Synthesis of Chiral 3,4-Dihydroisoquinolones. *J. Org. Chem.* **2019**, *84* (20), 12835−12847.
(15) Marrazzo, J.-P. R.; Chao, A.; Li, Y.; Fleming, F. F. Copper-Catalyzed Conjugate Additions to Isocyanoalkenes. *J. Org. Chem.* **2022**, *87* (1), 488−497.
(16) Jiang, X.; Han, B.; Xue, Y.; Duan, M.; Gui, Z.; Wang, Y.; Zhu, S. Nickel-Catalysed Migratory Hydroalkynylation and Enantioselective Hydroalkynylation of Olefins with Bromoalkynes. *Nat. Commun.* **2021**, *12* (1), No. 3792.
(17) Deng, Y.; Meng, Y.; Yang, Q.; Liu, Z.; Fan, R.; Chen, J.; Fan, B. Nickel/Copper Co-Catalyzed Enantioselective Reductive Coupling of Oxabenzonorbornadienes with Vinyl Bromides. *Adv. Synth. Catal.***2023** *n/a* (n/a). DOI: 10.1002/adsc.202300633.
(18) Bahamonde, A.; Al Rifaie, B.; Martín-Heras, V.; Allen, J. R.; Sigman, M. S. Enantioselective Markovnikov Addition of Carbamates to Allylic Alcohols for the Construction of α-Secondary and α-Tertiary Amines. *J. Am. Chem. Soc.* **2019**, *141* (22), 8708−8711.
(19) Guo, Z.-Q.; Xu, H.; Wang, X.; Wang, Z.-Y.; Ma, B.; Dai, H.-X. C3-Arylation of Indoles with Aryl Ketones via C−C/C−H Activations. *Chem. Commun.* **2021**, *57* (76), 9716−9719.
(20) Sietmann, J.; Tenberge, M.; Wahl, J. M. Wacker Oxidation of Methylenecyclobutanes: Scope and Selectivity in an Unusual Setting. *Angew. Chem., Int. Ed.* **2023**, *62* (7), No. e202215381.
(21) Ni, S.-X.; Li, Y.-L.; Ni, H.-Q.; Bi, Y.-X.; Sheng, J.; Wang, X.-S. Nickel-Catalyzed Hydromonofluoromethylation of Unactivated Alkenes for Expedient Construction of Primary Alkyl Fluorides. *Chin. Chem. Lett.* **2023**, *34* (3), No. 107614.
(22) Lux, M. C.; Boby, M. L.; Brooks, J. L.; Tan, D. S. Synthesis of Bicyclic Ethers by a Palladium-Catalyzed Oxidative Cyclization-Redox Relay-π-Allyl-Pd Cyclization Cascade Reaction. *Chem. Commun.* **2019**, *55* (49), 7013−7016.
(23) Race, N. J.; Schwalm, C. S.; Nakamuro, T.; Sigman, M. S. Palladium-Catalyzed Enantioselective Intermolecular Coupling of Phenols and Allylic Alcohols. *J. Am. Chem. Soc.* **2016**, *138* (49), 15881−15884.
(24) Chen, Z.-M.; Nervig, C. S.; DeLuca, R. J.; Sigman, M. S. Palladium-Catalyzed Enantioselective Redox-Relay Heck Alkynylation of Alkenols To Access Propargylic Stereocenters. *Angew. Chem., Int. Ed.* **2017**, *56* (23), 6651−6654.
(25) Zhang, C.; Santiago, C. B.; Crawford, J. M.; Sigman, M. S. Enantioselective Dehydrogenative Heck Arylations of Trisubstituted Alkenes with Indoles to Construct Quaternary Stereocenters. *J. Am. Chem. Soc.* **2015**, *137* (50), 15668−15671.
(26) Wang, M.-L.; Xu, H.; Li, H.-Y.; Ma, B.; Wang, Z.-Y.; Wang, X.; Dai, H.-X. Mizoroki−Heck Reaction of Unstrained Aryl Ketones via Ligand-Promoted C−C Bond Olefination. *Org. Lett.* **2021**, *23* (6), 2147−2152.
(27) Chen, J.; Li, J.-H.; Zhu, Y.-P.; Wang, Q.-A. Copper-Catalyzed Enantioselective Arylboronation of Activated Alkenes Leading to Chiral 3,3′-Disubstituted Oxindoles. *Org. Chem. Front.* **2021**, *8* (11), 2532−2536.
(28) Sandford, C.; Fries, L. R.; Ball, T. E.; Minteer, S. D.; Sigman, M. S. Mechanistic Studies into the Oxidative Addition of Co(I) Complexes: Combining Electroanalytical Techniques with Parameterization. *J. Am. Chem. Soc.* **2019**, *141* (47), 18877−18889.
(29) Yang, G.; Zhang, W. A Palladium-Catalyzed Enantioselective Addition of Arylboronic Acids to Cyclic Ketimines. *Angew. Chem., Int. Ed.* **2013**, *52* (29), 7540−7544.
(30) Zhou, B.; Li, K.; Jiang, C.; Lu, Y.; Hayashi, T. Modified Amino Acid-Derived Phosphine-Imine Ligands for Palladium-Catalyzed Asymmetric Arylation of Cyclic N-Sulfonyl Imines. *Adv. Synth. Catal.* **2017**, *359* (11), 1969−1975.
(31) Jiang, C.; Lu, Y.; Hayashi, T. High Performance of a Palladium Phosphinooxazoline Catalyst in the Asymmetric Arylation of Cyclic N-Sulfonyl Ketimines. *Angew. Chem., Int. Ed.* **2014**, *53* (37), 9936−9939.
(32) Li, M.-F.; Miao, A.-Q.; Zhu, H.-Y.; Wang, R.; Hao, W.-J.; Tu, S.-J.; Jiang, B. Palladium/N,N′-Disulfonyl Bisimidazoline-Catalyzed Enantioselective Addition of Arylboronic Acids to Cyclic N-Sulfonyl Ketimines. *J. Org. Chem.* **2020**, *85* (21), 13602−13609.
(33) Qiu, Z.; Li, Y.; Zhang, Z.; Teng, D. Spiro Indane-Based Phosphine−Oxazoline Ligands for Palladium-Catalyzed Asymmetric Arylation of Cyclic N-Sulfonyl Imines. *Transition Met. Chem.* **2019**, *44* (7), 649−654.
(34) Quan, M.; Yang, G.; Xie, F.; D Gridnev, I.; Zhang, W. Pd(Ii)-Catalyzed Asymmetric Addition of Arylboronic Acids to Cyclic N -Sulfonyl Ketimine Esters and a DFT Study of Its Mechanism. *Org. Chem. Front.* **2015**, *2* (4), 398−402.
(35) Álvarez-Casao, Y.; Monge, D.; Álvarez, E.; Fernández, R.; Lassaletta, J. M. Pyridine−Hydrazones as N,N′-Ligands in Asymmetric Catalysis: Pd(II)-Catalyzed Addition of Boronic Acids to Cyclic Sulfonylketimines. *Org. Lett.* **2015**, *17* (20), 5104−5107.
(36) Schrapel, C.; Peters, R. Exogenous-Base-Free Palladacycle-Catalyzed Highly Enantioselective Arylation of Imines with Arylboroxines. *Angew. Chem., Int. Ed.* **2015**, *54* (35), 10289−10293.
(37) Quan, M.; Wu, L.; Yang, G.; Zhang, W. Pd(II), Ni(II) and Co(II)-Catalyzed Enantioselective Additions of Organoboron Reagents to Ketimines. *Chem. Commun.* **2018**, *54* (74), 10394−10404.
(38) Jiang, T.; Wang, Z.; Xu, M.-H. Rhodium-Catalyzed Asymmetric Arylation of Cyclic N-Sulfonyl Aryl Alkyl Ketimines: Efficient Access to Highly Enantioenriched α-Tertiary Amines. *Org. Lett.* **2015**, *17* (3), 528−531.
(39) Nishimura, T.; Noishiki, A.; Chit Tsui, G.; Hayashi, T. Asymmetric Synthesis of (Triaryl)Methylamines by Rhodium-

Catalyzed Addition of Arylboroxines to Cyclic N-Sulfonyl Ketimines. *J. Am. Chem. Soc.* **2012**, *134* (11), 5056−5059.
(40) Döpp, D.; Lauterfeld, P.; Schneider, M.; Schneider, D.; Henkel, G.; Issac, Y. A. el S.; Elghamry, I. Photoisomerization of Sultams Derived from Saccharin; Part 4: Generation of Cyclic Sulfine Hydroxamic Acids. *Synthesis* **2001**, *112* (8), 1228−1235.
(41) Elghamry, I.; Döpp, D. A New Photochemical Ring Expansion of 1,2-Benzisothiazole 1,1-Dioxides. *Tetrahedron Lett.* **2001**, *42* (33), 5651−5653.
(42) Reddy, K. N.; Rao, M. V. K.; Sridhar, B.; Reddy, B. V. S. PdII-Catalyzed Spiroannulation of Cyclic N-Sulfonyl Ketimines with Aryl Iodides through C−H Bond Activation. *Eur. J. Org. Chem.* **2017**, *2017* (28), 4085−4090.
(43) Penso, M.; Albanese, D.; Landini, D.; Lupi, V.; Tagliabue, A. Complementary Heterogeneous/Homogeneous Protocols for the Synthesis of Densely Functionalized Benzo[d]Sultams: C−C Bond Formation by Intramolecular Nucleophilic Aromatic Fluorine Displacement. *J. Org. Chem.* **2008**, *73* (17), 6686−6690.
(44) Hallman, K.; Macedo, E.; Nordström, K.; Moberg, C. Enantioselective Allylic Alkylation Using Polymer-Supported Palladium Catalysts. *Tetrahedron: Asymmetry* **1999**, *10* (20), 4037−4046.
(45) Aranda, C.; Cornejo, A.; Fraile, J. M.; García-Verdugo, E.; Gil, M. J.; Luis, S. V.; Mayoral, J. A.; Martinez-Merino, V.; Ochoa, Z. Efficient Enhancement of Copper-Pyridineoxazoline Catalysts through Immobilization and Process Design. *Green Chem.* **2011**, *13* (4), 983−990.
(46) Bartáček, J.; Váňa, J.; Drabina, P.; Svoboda, J.; Kocúrik, M.; Sedlák, M. Recoverable Polystyrene-Supported Palladium Catalyst for Construction of All-Carbon Quaternary Stereocenters via Asymmetric 1,4-Addition of Arylboronic Acids to Cyclic Enones. *React. Funct. Polym.* **2020**, *153*, No. 104615.
(47) Lestini, E.; Blackman, L. D.; Zammit, C. M.; Chen, T.; Williams, R. J.; Inam, M.; Couturaud, B.; O'Reilly, R. K. Palladium-Polymer Nanoreactors for the Aqueous Asymmetric Synthesis of Therapeutic Flavonoids. *Polym. Chem.* **2018**, *9* (7), 820−823.
(48) Zhou, L.; Qiu, J.; Wang, M.; Xu, Z.; Wang, J.; Chen, T. Fabrication of Nanoreactors Based on End-Functionalized Polymethacrylate and Their Catalysis Application. *J. Inorg. Organomet. Polym. Mater.* **2020**, *30* (11), 4569−4577.
(49) Pezzetta, C.; Bonifazi, D.; Davidson, R. W. M. Enantioselective Synthesis of N-Benzylic Heterocycles: A Nickel and Photoredox Dual Catalysis Approach. *Org. Lett.* **2019**, *21* (22), 8957−8961.
(50) Moradi, W. A.; Schlegel, G.; Schnatterer, A.; Volz, F. Catalytic Hydrogenation of Substituted Cyanopyridines and Process for Preparing Substituted Pyridylmethylbenzamides. WO2016173998A1, November 3, 2016.
(51) Shen, G.; Osako, T.; Nagaosa, M.; Uozumi, Y. Aqueous Asymmetric 1,4-Addition of Arylboronic Acids to Enones Catalyzed by an Amphiphilic Resin-Supported Chiral Diene Rhodium Complex under Batch and Continuous-Flow Conditions. *J. Org. Chem.* **2018**, *83* (14), 7380−7387.

NOTE ADDED AFTER ASAP PUBLICATION

This paper was published ASAP on October 12, 2023 with errors in Figure 1 and an incorrect Figure 2 graphic. The corrected version was reposted on October 12, 2023.

https://doi.org/10.1021/acs.joc.3c01671
J. Org. Chem. 2023, 88, 15189−15197